THRUST ANALYSIS ON A SINGLE-DRIVE ROBOTIC FISH WITH AN ELASTIC JOINT

Yicun Xu[1]
Dongchen Qin[1]
[1]School of Mechanical Engineering
Zhengzhou University
No. 100, Kexue Road, Zhengzhou,
Henan, P.R. China. 450001

Cong Liu[2,3]
Houxiang Zhang[2]
[2]Faculty of Maritime Technology and Operation
Aalesund University College
Postboks 1517, N-6025 Aalesund,
Norway

[3]Department of Engineering Design and Materials,
Norwegian University of Science and Technology N-7491
Trondheim, Norway

KEYWORDS

Bionics, Robot fish, Thrust, Elastic joint, Simulation

ABSTRACT

This work simplified tuna’s swimming mode, then designed a single-drive robotic fish propulsion mechanism which including an elastic joint, and established the dynamics model of the mechanism. The thrust, resistance, resistance power on different peduncle oscillation parameters, and torsional stiffness of the caudal fin joint was simulated. The average thrust, maximum resistance and the average power grow with the increasing of the oscillating amplitude and the frequency. When the torsional stiffness of the caudal fin joint becomes larger, the thrust decreases, the resistance and the average power increase. The simulation results proved that the mechanism can generate thrust in water and it may be used as a robot fish propulsion mechanism.

INTRODUCTION

During millions of years of evolution, fishes have developed optimum body structures and appropriate swimming modes shaped by various environments. Their advantages in efficiency, low noise and maneuverability can potentially compensate the disadvantages of traditional propellers. Therefore, researchers have focused on the fish-mimicking mechanisms, with which the underwater vehicles can be propelled, target at developing a high performance robot fish.

Fishes’ swimming modes can basically be categorized into Body and/or Caudal Fin (BCF) locomotion and Median and/ or Paired Fin (MPF) locomotion (Sfakiotakis et al. 1999). Around 85% of fishes adopt BCF locomotion, swim by bending their bodies into a backward-moving wave which extends into its caudal fin (VIDELER, JJ .1993). According to the wavelength and the amplitude enveloped of the wave, the BCF mode is divided into four types: Anguilliform, Subcarangiform, Carangiform and Thunniform (C. C. Lindsey, 1978).

The main difference of the first three types is the characteristics of the body wave which produces the propulsive movement. By thunniform, the front part of the fish body can be basically regarded as rigid, propulsive movement is limited to the 1/3 rear part of the body, especially the caudal peduncle and caudal fin. The caudal fin generates more than 90% propulsion. This mode is suitable for a long-time and high-speed cruise. The fastest marine animals such as yellow-fin tunas represent thunniform. Tunas’ swimming speed can be up to 20 knots, and the propulsive efficiency can be as high as 80% or more (Tong Binggang 2000). Therefore, to mimic thunniform swimming is a hot spot in bionic robotic fish researches.
Stix in MIT carried out research on bionic robotic fish. By developing the first complete bionic robotic fish *Robotuna* (Stix, G. 1994). The length of *Robotuna* is about 1.2m. Japan's National Institute of Oceanography developed a thunniform bionic robotic fish, it’s length is

Proceedings 27th European Conference on Modelling and Simulation ©ECMS Webjørn Rekdalsbakken, Robin T. Bye, Houxiang Zhang (Editors)
ISBN: 978-0-9564944-6-7 / ISBN: 978-0-9564944-7-4 (CD)

about 1m, and the speed is up to 0.97m/s (www.nmri.go.jp). In China, Beihang University(BUAA) (Liang, J.et al. 2011.), Harbin Engineering University (Cheng Wei et al. 2004), Institute of Automation of Chinese Academy of Sciences(CAS) (Su, Z. et al. 2010) developed different prototypes of thunniform bionic robotic fishes. In order to mimic the oscillation of the caudal peduncle and caudal fin, these prototypes often use 2 or 3 motors as drivers. Both the structure and the control system are relatively complex.

In reality, the fish's flexible bodies can deform under the muscular driving force and the external forces. This makes it possible to generate the desired movements with fewer and simpler drives. Xu (XU et al. 2008, XU et al. 2007) applied this mechanism to the bionic flapping wing aircraft and a robotic fish with MPF swimming mode. Both of these approaches featured a single drive with flexible wings or fins.

In the following chapters, a single-drive bionic propulsive mechanism with an elastic joint was introduced. The propulsive mechanism was analyzed, and a simulation model was built. The relationship between thrust, resistance, power and the peduncle oscillation parameters, the torsional stiffness of the caudal fin joint was obtained by simulation. The simulation results proved the feasibility of such a propulsion mechanism.

MODEL

Model of the robot fish

A typical fish that adopts thunniform swimming mode oscillates the peduncle to lead the caudal fin. At the same time, the attack angle of the caudal fin is changing continuously. The phase of the leading edge is always ahead of the trailing edge (see figure 1). Hence the caudal fin obtained a forward thrust. During this process, the keys to the thrust are the oscillation of the caudal fin and the changing of the attack angle of the caudal fin.

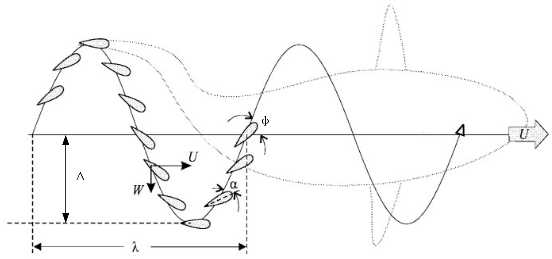

Figure 1 Thunniform swimming mode (adapted from Magnuson 1979)

In Figure 1, A tuna's body is divided into 3 parts for simplification: the body, the caudal peduncle and the caudal fin. The peduncle drives the caudal fin to oscillate, while the caudal fin deflects under the combined effect of hydrodynamic and inertial force. The phase of the leading edge is always ahead of the trailing edge.

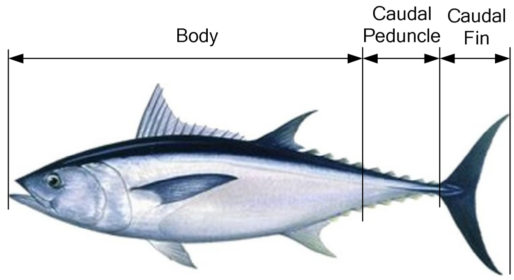

Figure 2 The three parts of a Tuna model

The mechanism in figure 3 is applied on robotic fish, mimicking tuna's swim motion. l stands for the length of peduncle, b indicates the length of the caudal fin, h represents the height of the caudal fin. The propulsion components consist of a body, a caudal peduncle and a caudal fin. The body and caudal peduncle is connected by an active joint, which is driven by a DC servo motor. The connection between caudal peduncle and caudal fin is made with a passive joint, with a tosional stiffness of k. The propulsion mechanism is shown as figure 3 and the simplified diagram is shown as figure 4. θ becomes the oscillation angle of peduncle, ϕ is obtained as the deflection angle, k is expressed as the torsional stiffness of the caudal fin joint. The caudal fin is designed in rectangle shape for simplification, instead of a crescent shape. The peduncle is designed with a length l, while the caudal fin has the length b and width h. The fluid drag and inertia force generated by peduncle is neglected.

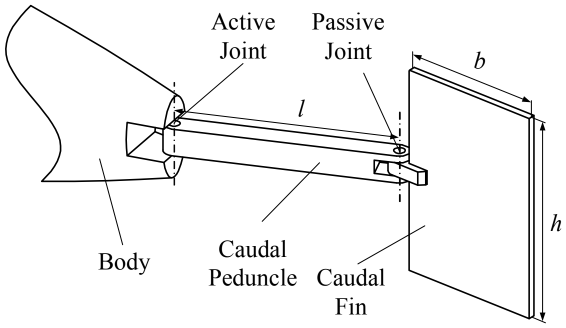

Figure 3 Propulsion mechanism of robot fish

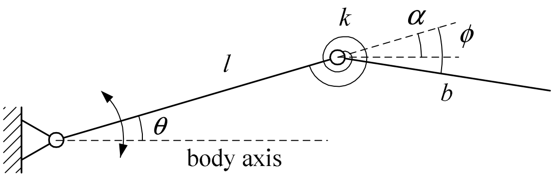

Figure 4 Simplified diagram of the propulsive mechanism

The angle of peduncle relative to the body axis can be written as

$$\theta = \theta_0 + A\sin(2\pi f t) \tag{1}$$

Where θ_0 is the neutral position of the peduncle oscillation, A and f respectively are the amplitude and the frequency.

$\dot{\theta}$ is the angular velocity of oscillation, and $\ddot{\theta}$ is the angular acceleration

Dynamics model of the mechanism

The change of equivalent length resulted by the rotation of caudal fin is neglected. Therefore, the induced velocity yields

$$v = \dot{\theta}\left(l + \frac{b}{2}\right) \tag{2}$$

Caudal fin coincides with peduncle. While the peduncle oscillating, the caudal fin starts to deflect under the hydrodynamic force and inertia force. The deflection angle ϕ, the actual angle of attack of the caudal fin can be derived as

$$\alpha = \theta + \phi \tag{3}$$

The inertia torque applied on caudal fin yields

$$F_{\mathrm{m}} = \ddot{\theta}\left(l + \frac{b}{2}\right)m \tag{4}$$

The resistant force applied on caudal fin yields

$$F_{\mathrm{D}} = \frac{1}{2}C_{\mathrm{D}}\rho S v^2 \cos\phi \tag{5}$$

The orientation of resistance is opposite to the direction of oscillation, where the area $S = bh$, C_{D} is drag coefficient. For a rectangular plate, the drag coefficient is assumed to range between 1.5 and 1.95.

After multiplying the drag and the induced velocity, and integrating in one oscillation period, the average driving power in one cycle is derived as

$$\overline{P_{\mathrm{D}}} = \frac{1}{T}\int_0^T F_{\mathrm{D}} v\,dt \tag{6}$$

The torque applied on the joint of caudal fin is

$$T_{\mathrm{k}} = F_{\mathrm{m}}\frac{b}{2} + F_{\mathrm{D}}\frac{b}{2}\cos\phi \tag{7}$$

The deflection angle of caudal fin is

$$\phi = \frac{T_{\mathrm{k}}}{k} \tag{8}$$

The thrust generated by caudal fin yields to

$$F_{\mathrm{T}} = \frac{1}{2}C_{\mathrm{D}}\rho S v^2 \sin\alpha \tag{9}$$

Simulation model

According to the equations, a simulation model as shown in figure 5 (Scilab, 2011) is built.

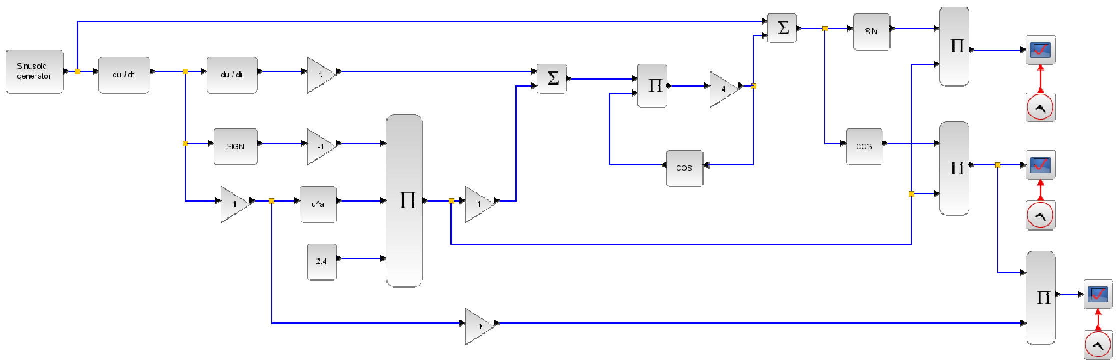

Figure 5 Simulation model

The parameters are listed in table 1.

Table1 Parameters in simulation

Parameter	Symbol	Value	Unit
Amplitude	A	π/18-2π/9	rad
Frequency	f	0.4-2	Hz
Length of caudal peduncle	l	0.1	m
Length of caudal fin	b	0.06	m
Width of caudal fin	h	0.05	m
Mass of caudal fin	m	0.02	kg
Density of water	ρ	1000	kg/m^3
Coefficient of drag	C_d	1.6	1
Torsional stiffness	k	0.2-1	rad /(Nm)

Simulation results

Figure 6, 7 and 8 separately show the thrust, resistance and resistance power versus oscillation angle in two cycles when $\mathrm{A} = \pi/9$, $f = 1\mathrm{Hz}$, $k = 0.1\mathrm{rad/(Nm)}$. In Figure 6, the thrust has two peaks during one cycle. Each peak occurs approximately when the maximum velocity of forward and backward exists.

According to equation (5) and (6), the thrust is related to the induced velocity v and the attack angel α. The oscillation velocity and the induced velocity reach their peaks simultaneously. The torque generated by resistance is largest. Hence, there is a peak of thrust.

Instantaneous negative thrust appears in the two oscillation limit positions. This is because of when the caudal fin near the limit positions, the induced velocity reduced. At the same time, the inertial force drives the position of trailing edge beyond the leading edge, a "negative attack angel" appears. Hence, there generated an instantaneous negative thrust.

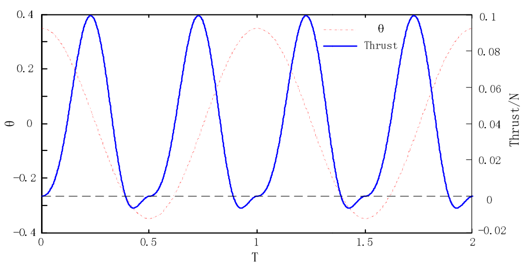

Figure 6 The curves of the oscillation angle and the thrust in two oscillation cycles.

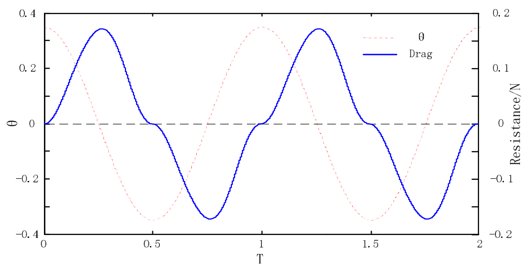

Figure 7 Curves of oscillation angle and resistance in two cycles.

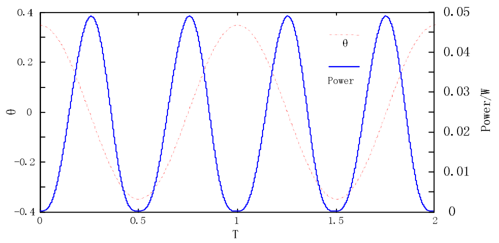

Figure 8 Average powers under different simulation parameters

Figure 9 to figure 11 show the average thrust, maximum resistance and the power in one cycle when oscillating amplitude A, oscillating frequency f and the torsional stiffness of the caudal fin joint k take different values.

With the increasing of oscillating amplitude A, oscillating frequency f, the induced velocity increases, hence the resistance, power and the thrust increase.

When the torsional stiffness k decreases, the same resistance moment leads a bigger deflection angle ϕ, then the resistance and the oscillating power decrease and the thrust increases. This seems like that decrease the torsional stiffness may improve efficiency. However, this model is based on a small deformation assumption, when torsional stiffness decrease to a certain limit, the small deformation assumption will hold no more, and mistakes will occur in simulation.

Analysis from the view point of the physical meaning, when deflection angle becomes larger, the effective area of the fin becomes smaller, there will be a decreasing trend of the resistance. And the decreased resistance limited the deflection angle further increase.

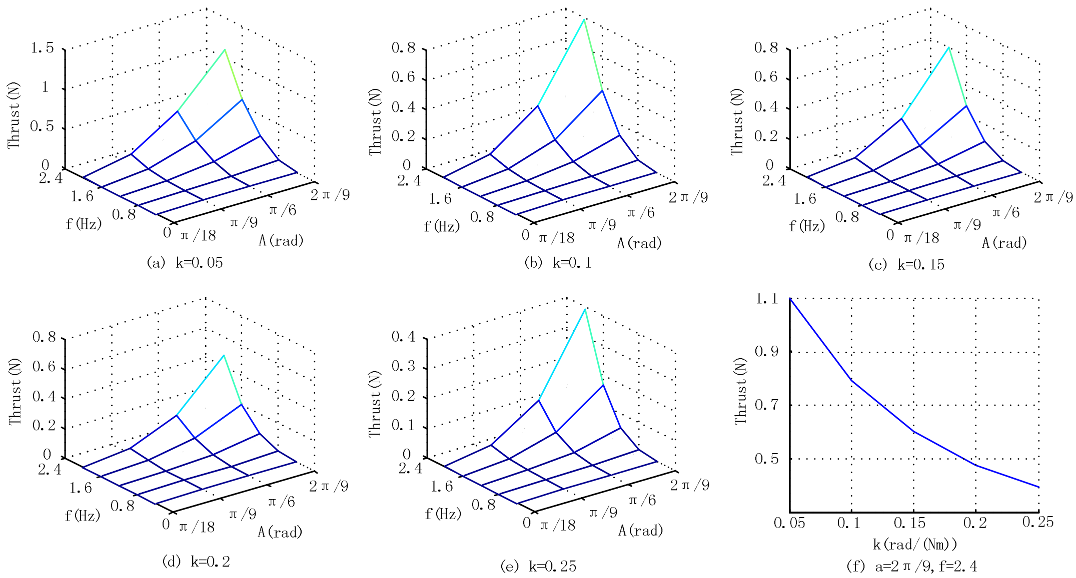

Figure 9 Average thrusts under different simulation parameters

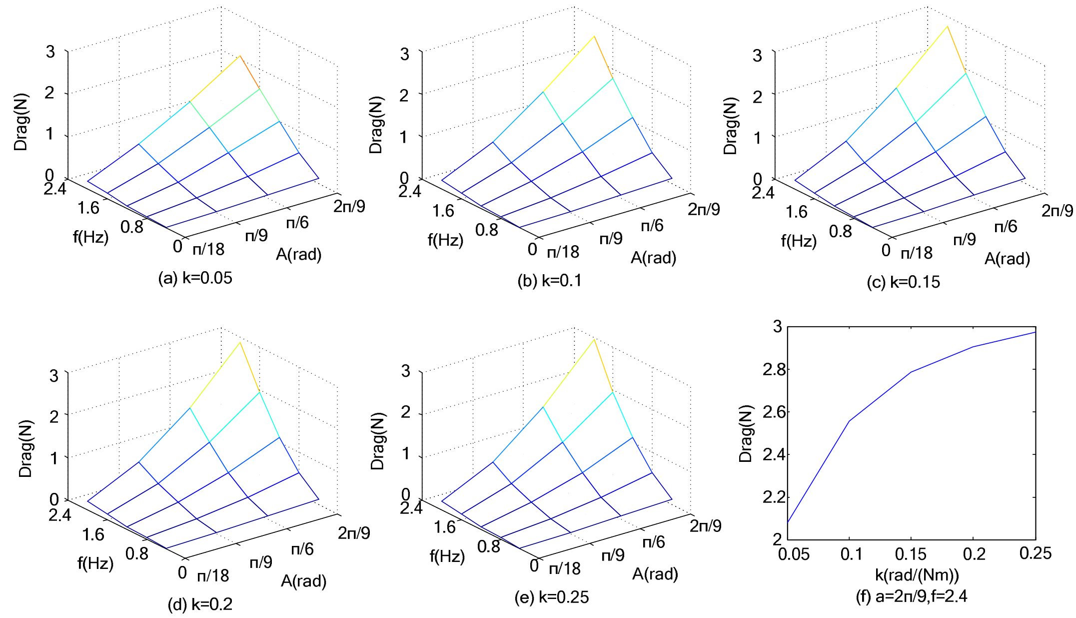

Figure 10 Maximum resistances under different simulation parameters

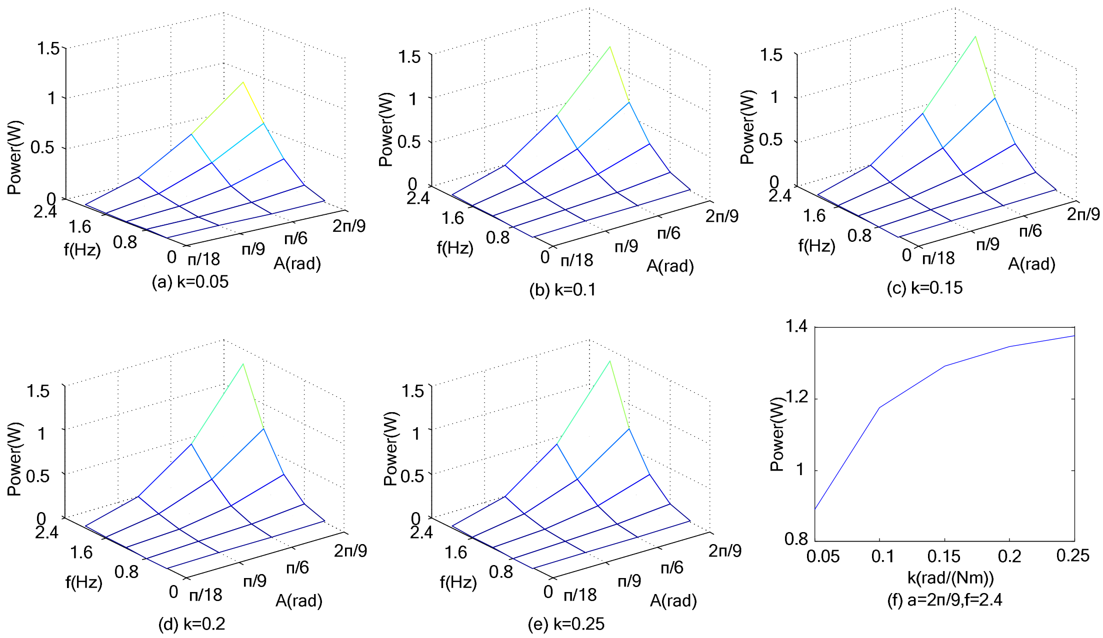

Figure 11 Average powers under different simulation parameters

SUMMARY

This paper aims to analyze Thunniform swimming mode by simplifying the motion of the tuna fish, a typical species of fish that adopts such swimming mode. A propulsion mechanism with a single drive and a flexible joint is then designed.

A dynamic model of the propulsion mechanism was established and simulated. The relationship between thrust, resistance, resistance power and the peduncle oscillation parameters, the torsional stiffness of the caudal fin joint was obtained by simulation. By observing the simulation data in one oscillation cycle, the oscillation resistance and the generated thrust have two peaks in one cycle. Both of the peaks occur when the fin is at neutral position. According to the simulation result under different simulation parameters, with the increasing of the oscillation and frequency, the average thrust, maximum resistance, average resistance power increase. With the increasing of the torsional stiffness of the caudal fin joint, the thrust decreases, the resistance and power increase.

The simulation result proved that such a mechanism may generate thrust in water and it may be used as the propulsive mechanism of a bionic robot fish.

REFERENCES

Sfakiotakis, Michael, David M. Lane, and J. Bruce C. Davies. 1999. "Review of fish swimming modes for aquatic locomotion. " *Oceanic Engineering*, IEEE Journal of 24, no. 2: 237-252
VIDELER, JJ .1993. “Fish Swimming”. London: Chapman and Hall.
C. C. Lindsey, “Form, function and locomotory habits in fish,” in Fish Physiology Vol. VII Locomotion, W. S. Hoar and D. J. Randall, Eds. New York: Academic, 1978, 1–100.
Tong Binggang. 2000. " Fish wavy swimming propulsion mechanism." *Mechanics in Engineering* 22, no. 3: 69-74. (In Chinese)
Stix, G. 1994. “RoboTuna”. *Scientific American*, 270, 142-142
http://www.nmri.go.jp/eng/khirata/fish/experiment/upf2001/index_e.html
Liang, J., Wang, T., & Wen, L. 2011. “Development of a two‐joint robotic fish for real‐world exploration”. *Journal of Field Robotics*, 28(1), 70-79
Cheng Wei, Su yumin, Qin Zaibai and Xu Yuru. 2004. “Development of a bionic underwater vehicle”. *Ship Engineering*, 26(1), 5-8. (In Chinese)
Su, Z., Yu, J., Tan, M., & Zhang, J. (2010, October). Closed-loop precise turning control for a BCF-mode robotic fish. *In Intelligent Robots and Systems (IROS)*, 2010 IEEE/RSJ International Conference on (pp. 946-951). IEEE
XU Yicun, BI Shusheng, ZONG Guanghua. 2008.” Thrust analysis and experimental study of the flexible wings of a flapping-wings aircraft”. *Journal of Aerospace Power*, 23(10), 1892-1895. (In Chinese)
Xu Yicun, Guanghua Zong, Shusheng Bi, and Jun Gao. 2007. "Initial development of a flapping propelled unmanned underwater vehicle (UUV)." *In Robotics and Biomimetics*. ROBIO 2007. IEEE International Conference on, pp. 524-529. IEEE, 2007
Magnuson, J. J. 1979. Locomotion by scombrid fishes: hydromechanics, morphology, and behavior. Fish physiology, 7, 239-313.
Scilab: Free and Open Source software for numerical computation (Windows Edition, Version 5.33) [Software]. Available from: http://www.scilab.org

AUTHOR BIOGRAPHIES

YICUN XU received his PhD in Robotics Institute, Beihang University at 2009. He works in School of Mechanical Engeering, Zhengzhou University since July 2009. Research field includes: biomimetic robotics, mechanical system dynamics.
Email: xuyicun@zzu.edu.cn

CONG LIU works in Aalesund University College as a PhD candidate since October 2011. He received his Master’s diploma in Mechanical Electronics Engineering from Beihang University in Beijing.
Email: lico@hials.no.

HOUXIANG ZHANG worked at the Institute of Technical Aspects of Multimodal Systems (TAMS), University of Hamburg from 2004 to 2011. Prof. Zhang joined Aalesund University College, Norway in 2011, focusing on Robotics and Cybernetics.
Email: hozh@hials.no.

DONGCHEN QIN recivied his PhD in Huazhong University of Scince and Technology at 2007. Work as a professr and deputy dean in School of Mechanical Engeering, Zhengzhou University. The mainly research field includes: Structural Optimization Design, Virtual Prototyping and Simulation, CAD/CAE/CAM System Integration.
Email:dcqin@zzu.edu.cn